

NASA-TP-3277 19920022036

**NASA  
Technical  
Paper  
3277**

August 1992

# Applications of FEM and BEM in Two-Dimensional Fracture Mechanics Problems

J. B. Min,  
B. E. Steeve,  
and G. R. Swanson

LIBRARY COPY

AUG 1 1992

LANGLEY RESEARCH CENTER  
LIBRARY NASA  
HAMPTON, VIRGINIA

**NASA**

**NASA  
Technical  
Paper  
3277**

1992

Applications of FEM and BEM  
in Two-Dimensional Fracture  
Mechanics Problems

J. B. Min,  
B. E. Steeve,  
and G. R. Swanson  
*George C. Marshall Space Flight Center  
Marshall Space Flight Center, Alabama*



National Aeronautics and  
Space Administration  
Office of Management  
Scientific and Technical  
Information Program

## TABLE OF CONTENTS

	Page
I. INTRODUCTION .....	1
II. FINITE ELEMENT METHOD .....	1
A. Elastic Analysis of a Single-Edge Crack .....	3
B. Elastic Analysis of an Inclined Crack .....	4
III. BOUNDARY ELEMENT METHOD .....	4
A. Elastic Analysis of a Single-Edge Crack .....	6
B. Elastic Analysis of an Inclined Crack .....	6
IV. RESULTS AND CONCLUSIONS .....	7
REFERENCES .....	17

## LIST OF ILLUSTRATIONS

Figure	Title	Page
1.	Local coordinates measured from a two-dimensional crack tip .....	8
2.	Nodes used for the approximate crack-tip displacements: (a) full model and (b) half model .....	9
3.	A single-edge crack in a plate under tension .....	10
4.	$\sigma_y$ (lb/in <sup>2</sup> ) on deformed shape .....	11
5.	Inclined-edge crack under tension .....	12
6.	$\sigma_y$ (lb/in <sup>2</sup> ) on deformed shape .....	13
7.	Arbitrary loaded component .....	14
8.	Deformed shape on original shape .....	15
9.	Deformed shape on original shape .....	16

## TECHNICAL PAPER

# APPLICATIONS OF FEM AND BEM IN TWO-DIMENSIONAL FRACTURE MECHANICS PROBLEMS

## I. INTRODUCTION

The finite element method (FEM) and boundary element method (BEM) are widely employed in fracture mechanics.<sup>1-6</sup> Both methods are employed for fracture mechanics problems, but neither method is effective and accurate for all fracture problems. Judging the effectiveness and accuracy of FEM or BEM requires practical experience in the field. Traditionally, the stress analysis has used the FEM. However, the fracture mechanics problems have crack edge boundary and singular points at the crack tip which are inconvenient to mesh because full domain discretization is required. In addition, around crack tips, extremely fine subdivisions are required to achieve reasonable accuracy. It takes quite a length of time for an engineer to build and check such a model. It has been proposed that these disadvantages are overcome by the BEM since the elements are placed only on the boundary of the domain. However, this method also has difficulty in mathematical degeneracy and the treatment of nonlinearities. A number of different approaches have been developed to address the problem of degeneracies. Also, in order to overcome the disadvantages of these methods, coupled finite element—boundary element methods have been developed.<sup>7</sup>

The objective of this paper is not to make a judgment on these methods but, to show how the FEM and BEM can be employed in fracture mechanics problems and also to find how both methods can be used in practical applications, such as analyzing component failure in aerospace structures caused by fracture and fatigue.

## II. FINITE ELEMENT METHOD

Since several excellent and comprehensive works explaining basic fracture mechanics theory are readily available in the literature,<sup>7-12</sup> a comprehensive review is not made here. However, selected features of the fundamental theory are reviewed. A critical step in modeling fracture problems is the selection of the type of element used to represent the singular region surrounding the crack tip. If regular (i.e., nonsingular) elements with polynomial displacement functions are selected, the convergence rate, based on element size, is very slow.<sup>13</sup> Moreover, the convergence rate at a singularity cannot be increased by merely selecting higher order polynomial elements. The ANSYS six-node triangular element with mid-side nodes at the quarter points was selected for the crack tip since it accurately models the singularity.<sup>14</sup> The rest of the domain was meshed with standard six-node triangular elements. The development of the singular isoparametric element is well documented in the literature.<sup>1 6 15-19</sup> The stress intensity factors were calculated from the nodal displacements, using the same techniques as the BEM models discussed in section III. The crack-tip near-field displacements and stresses for mode I behavior (the opening mode) and mode II (the shearing mode) are expressed in equations (1) and (2) in the crack-tip coordinates which are shown in figure 1.<sup>10</sup>

$$\begin{aligned}
u &= \frac{K_I}{4G} \sqrt{\frac{r}{2\pi}} \left[ (2\kappa-1) \cos \frac{\theta}{2} - \cos \frac{3\theta}{2} \right] - \frac{K_{II}}{4G} \sqrt{\frac{r}{2\pi}} \left[ (2\kappa+3) \sin \frac{\theta}{2} + \sin \frac{3\theta}{2} \right] + O(r) \\
v &= \frac{K_I}{4G} \sqrt{\frac{r}{2\pi}} \left[ (2\kappa-1) \sin \frac{\theta}{2} - \sin \frac{3\theta}{2} \right] + \frac{K_{II}}{4G} \sqrt{\frac{r}{2\pi}} \left[ (2\kappa-3) \cos \frac{\theta}{2} + \cos \frac{3\theta}{2} \right] + O(r) ,
\end{aligned} \tag{1}$$

and

$$\begin{aligned}
\sigma_x &= \frac{K_I}{\sqrt{2\pi r}} \left( 1 - \sin \frac{\theta}{2} \sin \frac{3\theta}{2} \right) \cos \frac{\theta}{2} - \frac{K_{II}}{\sqrt{2\pi r}} \left( 2 + \cos \frac{\theta}{2} \cos \frac{3\theta}{2} \right) \sin \frac{\theta}{2} + O(1) , \\
\sigma_y &= \frac{K_I}{\sqrt{2\pi r}} \left( 1 + \sin \frac{\theta}{2} \sin \frac{3\theta}{2} \right) \cos \frac{\theta}{2} + \frac{K_{II}}{\sqrt{2\pi r}} \sin \frac{\theta}{2} \cos \frac{3\theta}{2} + O(1) , \\
\sigma_z &= 0 \text{ for plane stress conditions} \\
&= \nu(\sigma_x + \sigma_y) \text{ for plane strain conditions} ,
\end{aligned} \tag{2}$$

$$\tau_{xy} = \frac{K_I}{\sqrt{2\pi r}} \sin \frac{\theta}{2} \cos \frac{\theta}{2} \cos \frac{3\theta}{2} + \frac{K_{II}}{\sqrt{2\pi r}} \left( 1 - \sin \frac{\theta}{2} \sin \frac{3\theta}{2} \right) \cos \frac{\theta}{2} + O(1) .$$

in which  $K_I$  and  $K_{II}$  are the stress intensity factors associated with mode I and mode II, respectively, of linear elastic fracture mechanics (LEFM).  $\sigma_x$ ,  $\sigma_y$ , and  $\tau_{xy}$  are the stress components in the rectangular  $(x,y,z)$  coordinate system;  $u$  and  $v$  are the displacements;  $r$  and  $\theta$  are local polar coordinates;  $G$  is the shear modulus; and  $\nu$  is Poisson's ratio. The variable  $\kappa$  is a conversion factor between plane strain and plane stress, where

$$\begin{aligned}
\kappa &= 3-4\nu \text{ for plane strain} \\
&= \frac{3-\nu}{1+\nu} \text{ for plane stress} .
\end{aligned} \tag{3}$$

The evaluating procedure for  $K_I$  and  $K_{II}$  from the finite element nodal displacements is not new<sup>17 20 21 23</sup> and neglecting higher order terms,

$$\begin{aligned}
u &= \frac{K_{II}}{G} \sqrt{\frac{r}{2\pi}} (1+\kappa) \\
v &= \frac{K_I}{G} \sqrt{\frac{r}{2\pi}} (1+\kappa) ,
\end{aligned} \tag{4}$$

where only the absolute value of displacement is considered.

Thus, the full opening and shearing displacements across the faces of the crack are obtained as follows:

$$\begin{aligned}
\Delta u &= \frac{K_{II}}{2G} \sqrt{\frac{r}{2\pi}} (1+\kappa) \\
\Delta v &= \frac{K_I}{2G} \sqrt{\frac{r}{2\pi}} (1+\kappa) ,
\end{aligned} \tag{5}$$

The method to extract  $K_I$  from mode I displacements is described here since the procedure is identical for  $K_{II}$ . In this case, the behavior of either  $\hat{v}(r)$  in equation (4) or  $\Delta\hat{v}(r)$  in equation (5) is approximated. On the crack face, it can be written

$$\frac{\hat{v}}{\sqrt{r}} \text{ or } \frac{\Delta\hat{v}}{\sqrt{r}} = A + Br , \quad (6)$$

where  $\hat{v}$  and  $\Delta\hat{v}$  are the approximations to the crack-face displacements, and  $A$  and  $B$  are constants determined from a linear curve fit of nodal displacements. All displacements are relative to the crack-tip node. Substituting the values of  $v$  or  $\Delta v$  and  $r$  for nodal points along a radial line emanating from the crack tip allows a plot of equation (6) against radial distance  $r$  to be drawn as shown in figure 2. Then by discarding the results for points very close to the crack tip, the solutions can be extrapolated to  $r = 0$ . Once  $A$  and  $B$  are determined, then the limit is found as  $r \rightarrow 0$ .

$$\lim_{r \rightarrow 0} \frac{\hat{v}}{\sqrt{r}} \text{ or } \lim_{r \rightarrow 0} \frac{\Delta\hat{v}}{\sqrt{r}} = A . \quad (7)$$

Solving first equation (4) and then equation (5) for  $K_I$  and combining with equation (7),

$$K_I = \frac{2G\sqrt{2\pi}A}{(1+\kappa)} \text{ for half-crack models} \quad (8)$$

$$K_I = \frac{G\sqrt{2\pi}A}{(1+\kappa)} \text{ for full-crack models .}$$

Using these steps, a single-edge crack and an inclined-edge crack in an elastic plate were solved and the results are described in the following subsections.

### A. Elastic Analysis of a Single-Edge Crack

The two-dimensional plate geometry is shown in figure 3, and the plane strain assumptions are used in this example. The model is symmetric about the  $y = 0$  axis, and the  $x$ -displacement at  $x = 0$  and  $y = 0$  was restrained to prevent rigid body translation. The dimensions used were  $a/b = 1$  and  $c/a = 6$ , where  $a$  is the crack length, and  $b$  and  $c$  are plate dimensions. A uniform tensile stress,  $\sigma$ , is applied at the ends of the plate. Material properties are Young's modulus of  $10 \times 10^6$  lb/in<sup>2</sup> and Poisson's ratio of 0.333. The theoretical stress intensity factor,  $K_I$ , associated with the crack-opening mode is expressed as

$$K_I = \sigma \sqrt{\pi a} \cdot f(a/b) , \quad (9)$$

where  $f(a/b)$  is a geometric correction factor. For  $a/b$ , a nearly exact solution is  $f(a/b) = 2.82$ .<sup>10</sup> It is convenient to rewrite equation (9) in dimensionless form:

$$\bar{K}_I = \frac{K_I}{\sigma \sqrt{\pi a}} = f(a/b) . \quad (10)$$

This leads to  $\bar{K}_I = 2.82$  as the exact solution to compare to the finite element results. In the model, six-node triangular elements are used except for eight singular elements placed at the tip of the crack. Also, only half the plate is modeled because of symmetry along the direction of the crack. The analysis results

are given in figure 4 and table 1 and indicate favorable agreement with the exact solution. Also, since most real engineering fracture problems involve more than a single mode of fracture, the next problem attempted was an inclined-edge cracked plate.

### B. Elastic Analysis of an Inclined Crack

An elastic two-dimensional plate, weakened by the presence of an inclined edge crack as shown in figure 5, was selected to extract the  $K_I$  and  $K_{II}$  stress intensity factors under plane strain assumptions. The boundary conditions are  $v = 0$  along the  $x$ -axis and  $u = 0$  at the point  $(0,0)$ . The dimensions used were  $a/w = 0.3$  and  $L/w = 5.0$  where  $a$  is crack length,  $w$  is plate width, and  $L$  is plate length. The crack is inclined  $45^\circ$ . The plate is subjected to a tensile stress ( $\sigma$ ) at its ends that will induce crack face opening (mode I) and crack face shearing (mode II). Since no planes of symmetry exist, a full model was generated with six-node triangular elements and singular elements placed in the crack-tip region. The analysis results are shown in figure 6 and table 1. Having the crack faces defined as shown in figure 2, the values of  $\bar{K}_I = 1.56$  and  $\bar{K}_{II} = 0.786$  were obtained. The theoretical values reported by Wilson<sup>22</sup> are 1.58 and 0.782, respectively.

## III. BOUNDARY ELEMENT METHOD

The BEM has been developed by a number of researchers, and recently a great deal of interest has been focused on this method as a complement to the FEM.<sup>24</sup> Although this technique offers accurate results with significant savings in time and/or cost, the range of practical applications is currently not as wide as the finite element technique. One area that has been identified as being well-suited for boundary element analysis is fracture mechanics since it only requires discretization of the surface rather than the volume. The simplified theory of the BEM follows:<sup>25</sup>

Take a component with volume  $\Omega$  and boundary  $\Gamma$  (fig. 7). The component is subjected separately to two load cases:

Load case 1: Loads  $t$ , Displacements  $u$

Load case 2: Loads  $t^*$ , Displacements  $u^*$ .

The reciprocal theorem states that the work done by the loads from load case 1 on the displacements from load case 2 is equal to the work done by the load case 2 on the displacements from load case 1. To find the work, we simply integrate over the body, so we can write

$$\int_{\Omega} t \cdot u^* d\Omega = \int_{\Omega} t^* \cdot u d\Omega . \quad (11)$$

Assuming that there are no body loads, the loading is confined to the boundary  $\Gamma$ , so the volume integrals may be rewritten as surface integrals. Body forces may still be considered in the BEM by using a Green's function to transform the volume integral term to a boundary integral. Rewriting as surface integrals,

$$\int_{\Gamma} t \cdot u^* d\Gamma = \int_{\Gamma} t^* \cdot u d\Gamma . \quad (12)$$



Now we specify that load case 1 represents the actual loading for which the analysis is performed. Load case 2, still being arbitrary, can be chosen to be anything we want to make the equations easier to handle. In practice, it turns out to be best to apply a point force at the node locations (like finite elements, boundary elements have nodes at which the equations are formed). We know the terms  $t^*$  and  $u^*$  from classical solutions. It is usual to call  $u^*$  “essential” and  $t^*$  “natural” boundary conditions.

Integrating the terms  $t$  and  $u$  numerically over the elements, a system of equations is formed in terms of the nodal displacements and loads

$$[H] [U] = [G] [T] , \quad (13)$$

where  $[H]$  and  $[G]$  are two  $N \times N$  matrices and  $[U]$  and  $[T]$  are vectors of length  $N$ .

The square matrix  $[H]$  is filled with the integrals of the  $t^*$  terms, and the square matrix  $[G]$  is filled with the integrals of the  $u^*$  terms. The vector  $[T]$  contains the unknown loads and the vector  $[U]$  contains the unknown displacements. This leaves us with  $N$  equations, but  $2N$  unknowns. However, since displacements (i.e.,  $u^*$ ) on  $\Gamma_1$  and tractions (i.e.,  $t^*$ ) on  $\Gamma_2$  are known, there are only  $N$  unknowns in the system of equation (13). To introduce these boundary conditions into equation (13), one has to rearrange the system by moving columns  $[H]$  and  $[G]$  from one side to the other. Once all unknowns are passed to the left-hand side, one can write,

$$[A] [X] = [F] , \quad (14)$$

where  $[X]$  is a vector of unknowns  $u$  and  $t$  boundary values.  $[F]$  is now all known.

This gives a familiar looking equation which may be solved by any standard matrix equation solver. Once the boundary solution has been found, it is possible to calculate any internal value of  $u$  or its derivatives. The values of  $u$  are calculated at any internal point “ $i$ ” using the formula which can be written as,

$$u^i = \int_{\Gamma} t \cdot u^* d\Gamma - \int_{\Gamma} u \cdot t^* d\Gamma . \quad (15)$$

Notice that now the fundamental solution is considered to be acting on an internal point “ $i$ ” and that all values of  $u$  and  $t$  are already known. The process is then one of integration (usually numerically). The stress and displacement at any given point internal to the material can be found by a similar integration procedure.

Although the theory underlying the BEM is relatively complicated, model creation is relatively simple because only the boundary needs to be defined. The details of modeling crack tips with boundary elements varies according to the software chosen. The Boundary Element Analysis System (BEASY) was used for this analysis. The following description is based on the BEASY code. In BEASY models, line elements are used for two-dimensional problems. The points which define the geometry of these elements are called “mesh points.” Unlike the FEM, these mesh points do not necessarily coincide with the “nodes,” at which the equations are formed for the results. It is necessary to make the distinction between mesh points and nodes. Mesh points define only the geometry, and the nodes define the

location where the values of displacement, temperature, etc., on the element are calculated. In most instances, the nodes are located at the mesh points for continuous elements. But when discontinuous elements are needed (as is the case for a discontinuous stress field at a crack tip), the nodes are located away from the mesh point. The number of nodes on an element varies according to the user's requirements. Quadratic elements were used in this study. The nodal results were calculated and then extrapolated to the mesh points. Mesh points are always at the middle and ends of two-dimensional elements and are shared wherever possible between adjacent elements. The extrapolation of results to a mesh point done by fitting a quadratic curve through the three nodal results can, therefore, be done from two or more elements. These mesh point results are, therefore, the mean values of the results obtained from the different elements connected to a mesh point.

As shown in figures 8 and 9, the models are meshed with graded element sizes. No special elements need to be defined at a crack-tip, but smaller elements are needed. In the region approaching a crack tip, the stress is varying very rapidly, and it is, therefore, important to use small elements. Use of such small elements throughout the model, though, would create too many elements to be run practically, so they should be graded out to larger elements in other parts of the model. However, if run time is not a dominating factor, then users can define very small elements at the crack tip. It should also be noted that a boundary element model can only model accurately if the elements are not required to model stress variation of a higher order than the elements themselves. For example, a quadratic element will be accurate only if the stress does not vary as a cubic function (or higher) over the length of the element.

The stress intensity factors are calculated using Irwin's equations<sup>26</sup> from both stress and displacement. The latter have been found to give consistently more accurate results. This is perhaps due to the fact that stress becomes singular at the crack-tip, whereas displacement does not. Notice that these equations are not valid at the crack tip. By extrapolating these values to the crack tip itself, the user can obtain an accurate estimate of the true stress intensity factor. In this study, the stress intensity factors were normalized as defined in section II. The same models solved in section II were modeled by BEASY and the results were obtained as follows.

#### **A. Elastic Analysis of a Single-Edge Crack**

The exact same model used for the finite element analysis shown in figure 3 was used for the boundary element analysis. The model contained 65 line elements. Only the top half of the plate was modeled due to the symmetry. Figure 8 illustrates the BEASY model of this problem. Following the analysis, a plot of the deformed shape was made, and the crack opening was observed as shown in this figure. The normalized  $K_I$  factor was obtained by the method described above, and the value of  $\bar{K}_I$  was 2.88. The result was then compared to the solution given in reference 10. The difference was approximately 2.1 percent. The theoretical value reported by Paris and Sih<sup>10</sup> is 2.82.

#### **B. Elastic Analysis of an Inclined Crack**

A crack developing from the edge of a plate at 45° to the plate edge is shown in figure 5. The whole plate was modeled using BEM because of no symmetry. In this case, the shear mode (mode II) acts in addition to the crack opening mode (mode I), therefore both  $K_I$  and  $K_{II}$  were calculated. The model consisted of 114 elements, and gave the values of  $\bar{K}_I = 1.57$  and  $\bar{K}_{II} = 0.794$ . The results were then compared to those obtained by Wilson.<sup>22</sup> The difference was less than 2 percent as shown in table 1. The theoretical values reported by Wilson<sup>22</sup> are 1.58 and 0.782, respectively. The deformed shape on the original shape is shown in figure 9.

#### IV. RESULTS AND CONCLUSIONS

Application of the FEM and BEM is just beginning for fracture mechanics analysis in the aerospace industry. Traditional methods/handbook solutions are still the predominate techniques used. However, these traditional techniques have limitations to simulate the practical cases. Therefore, the FEM and BEM have been considered and developed to resolve the limitation of traditional methods. However, the FEM is expensive in both manpower and computer costs, and cost saving alternatives are always being sought. The BEM has been considered to be one of them.

The single edge cracked plate and inclined edge cracked plate were analyzed with both the BEASY boundary element code and the ANSYS finite element code to see the relative strengths and weaknesses of both methods. Stress intensity factor calculations were computed on all the finite element models and boundary element models using the displacement extrapolation method. Final calculations for the stress intensity factors for the  $r$  fit are given in table 1. The boundary element  $K$  predictions were within 2 percent of the finite element  $K$  predictions. The agreement between the boundary element model and the finite element model is encouraging considering the difference in number of degrees of freedom (DOF) (1,250 with FEM to 266 with BEM for single edge crack case, 2,226 with FEM to 536 with BEM for inclined edge crack case). However, from a simple comparison of the solution times, the BEM (BEASY code) does not show more efficiency than the FEM (ANSYS code) as can be seen in table 1. For this comparison, a VAX/785 computer system was used. The most probable reason for this is that the boundary element model uses a "full" matrix without the banded symmetry common to the FEM. In other words, the relationship between matrix size, fullness, and the central processing unit (CPU) time to invert and solve the equations might be the reason for the efficiency in computing time. The FEM was more accurate than the BEM for the single edge crack problem. However, the  $K_I$  from the BEM was more accurate than that from the FEM, and the  $K_{II}$  from the FEM was more accurate than that from the BEM for the inclined edge crack problem. The most significant observation was that both methods provided a good correlation with the theoretical predictions, but about the same amount of modeling time was required to achieve favorable agreement with the exact solutions using both methods.

Table 1. Comparison of FEM and BEM.

Method	Case	Single Edge	Inclined Edge
FEM	Number of Elements	292	526
	Sol. Time CPU	190.15 s	384.85 s
	$K_I$	2.83	1.565
	Percent $\Delta$	0.4 percent	-0.95 percent
	$K_{II}$	—	0.7857
	Percent $\Delta$	—	0.47 percent
	DOF	1,250	2,226
BEM	Number of Elements	65	114
	Sol. Time CPU	254.30 s	727.50 s
	$K_I$	2.88	1.570
	Percent $\Delta$	2.1 percent	-0.6 percent
	$K_{II}$	—	0.794
	Percent $\Delta$	—	1.5 percent
	DOF	266	536
Ref.	$K_I$	2.82 [10]	1.58 [22]
	$K_{II}$	—	0.782 [22]

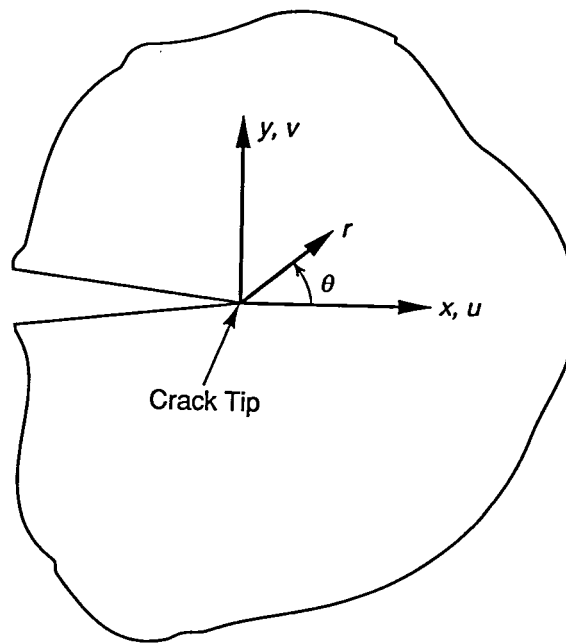
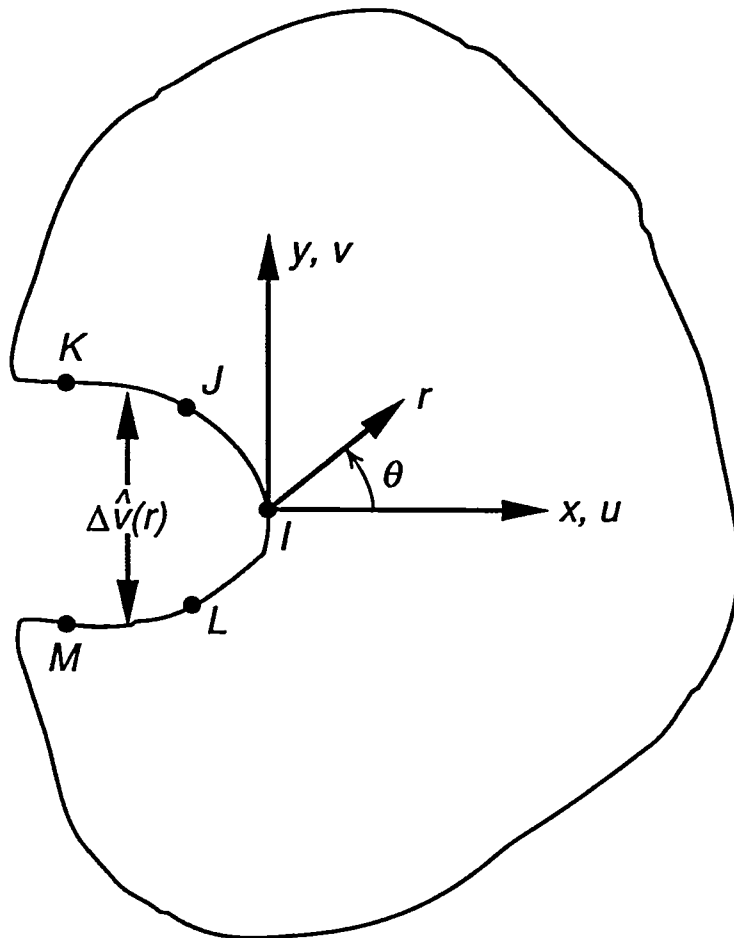


Figure 1. Local coordinates measured from a two-dimensional crack tip.

(a)



(b)

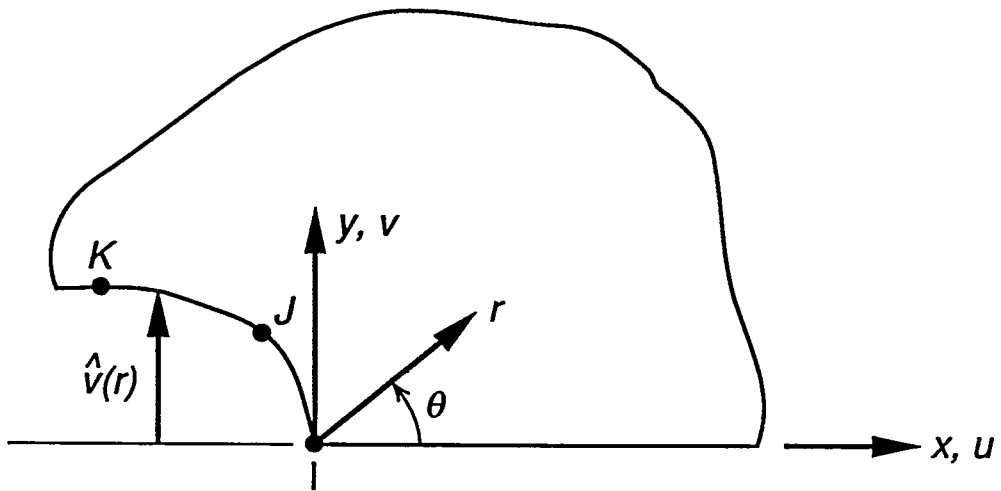


Figure 2. Nodes used for the approximate crack-tip displacements: (a) full model and (b) half model.

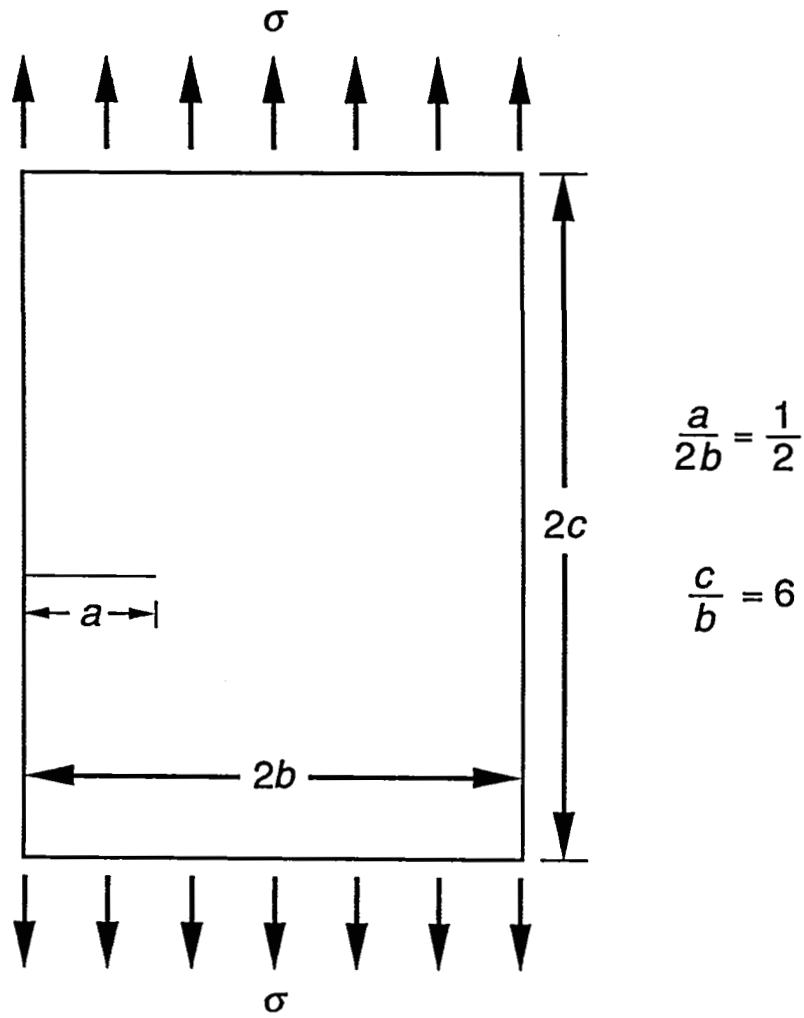


Figure 3. A single-edge crack in a plate under tension.

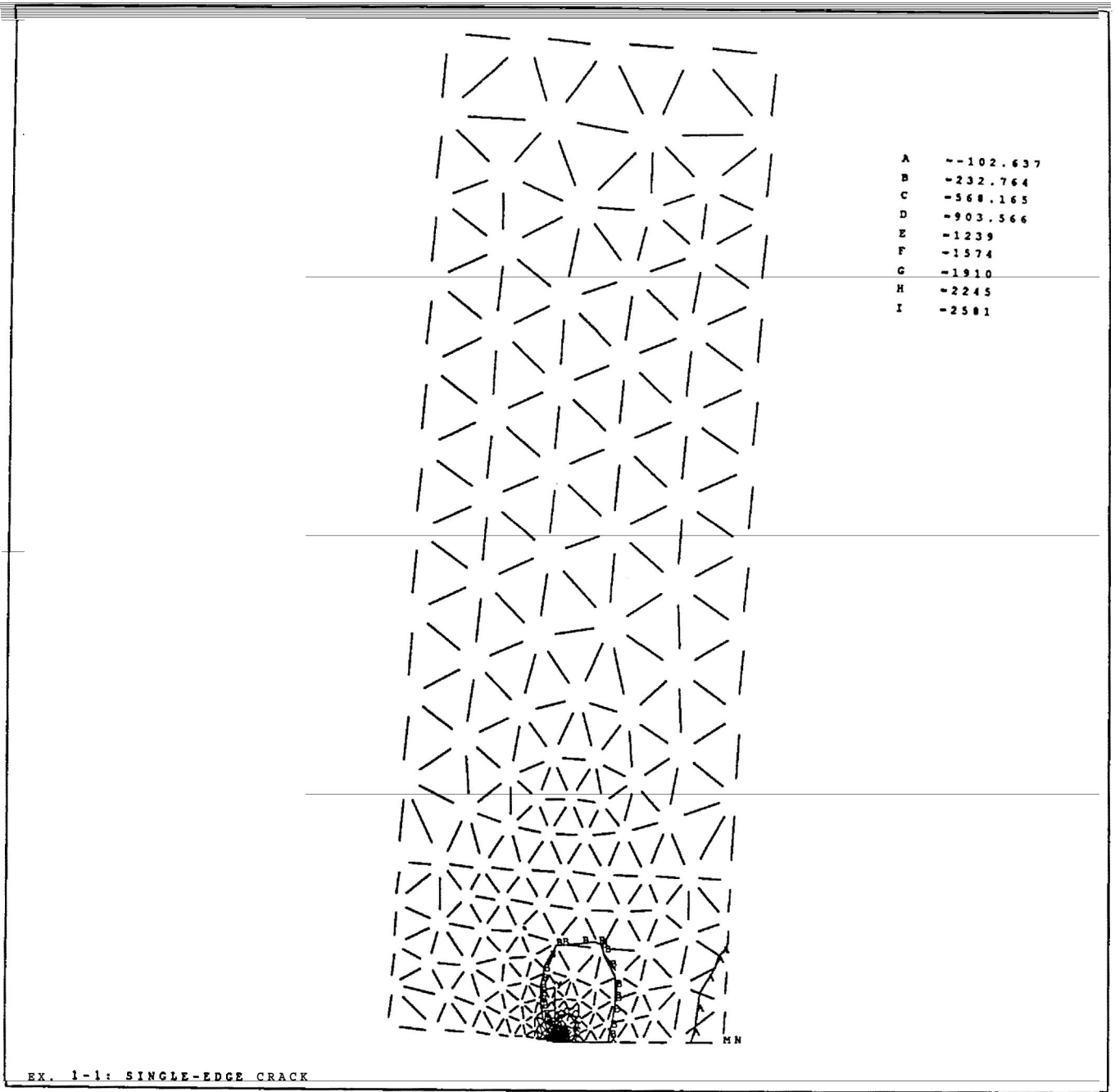


Figure 4.  $\sigma_y$  (lb/in<sup>2</sup>) on deformed shape.

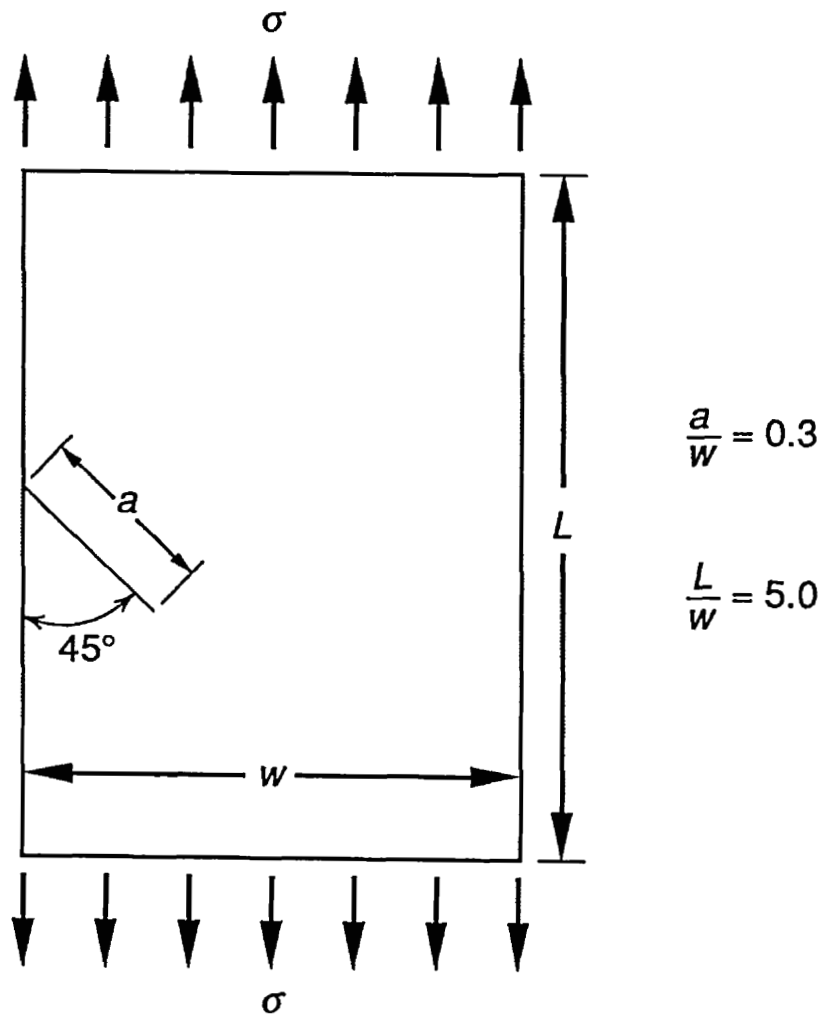


Figure 5. Inclined-edge crack under tension.



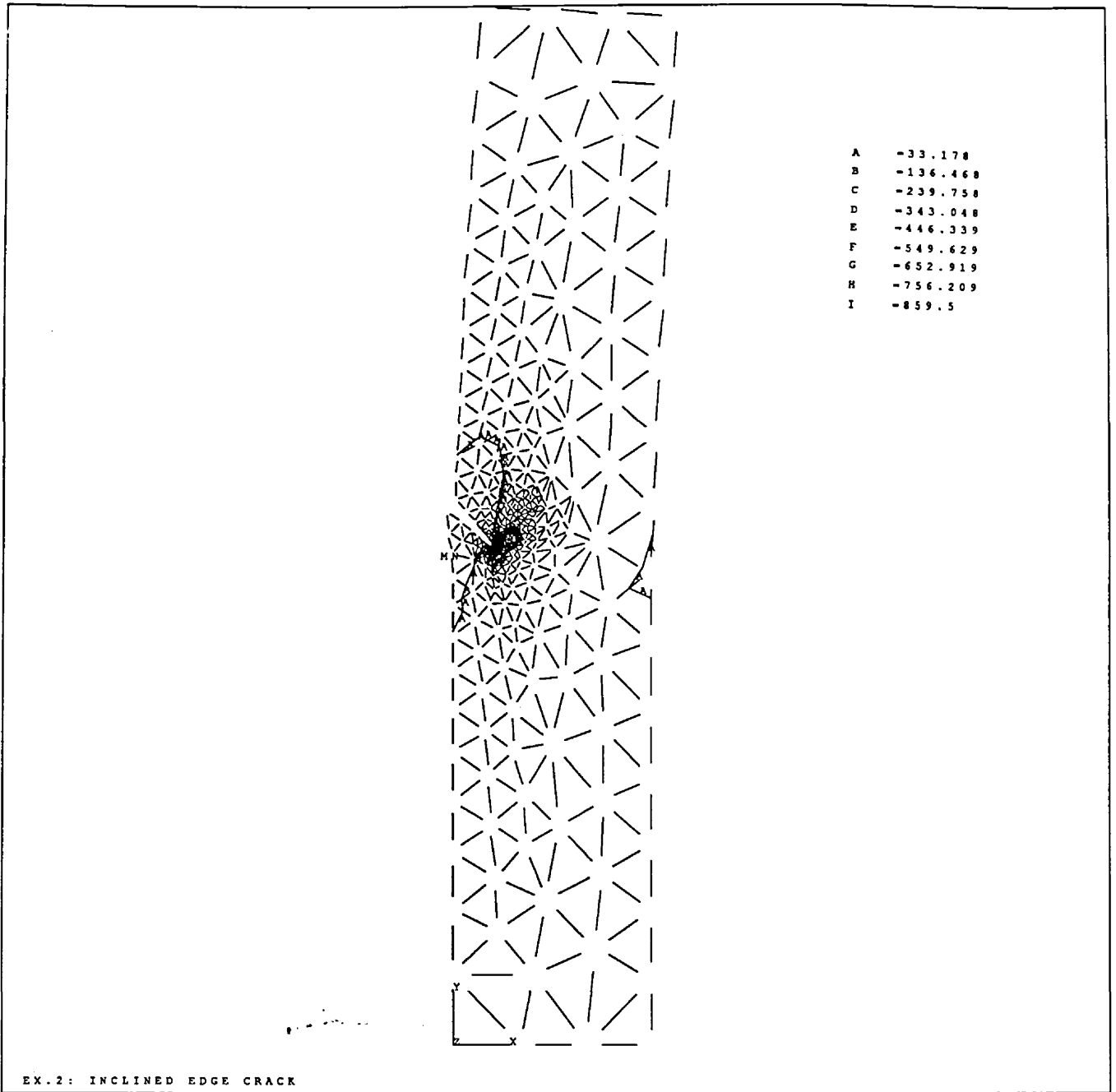


Figure 6.  $\sigma_y$  (lb/in<sup>2</sup>) on deformed shape.

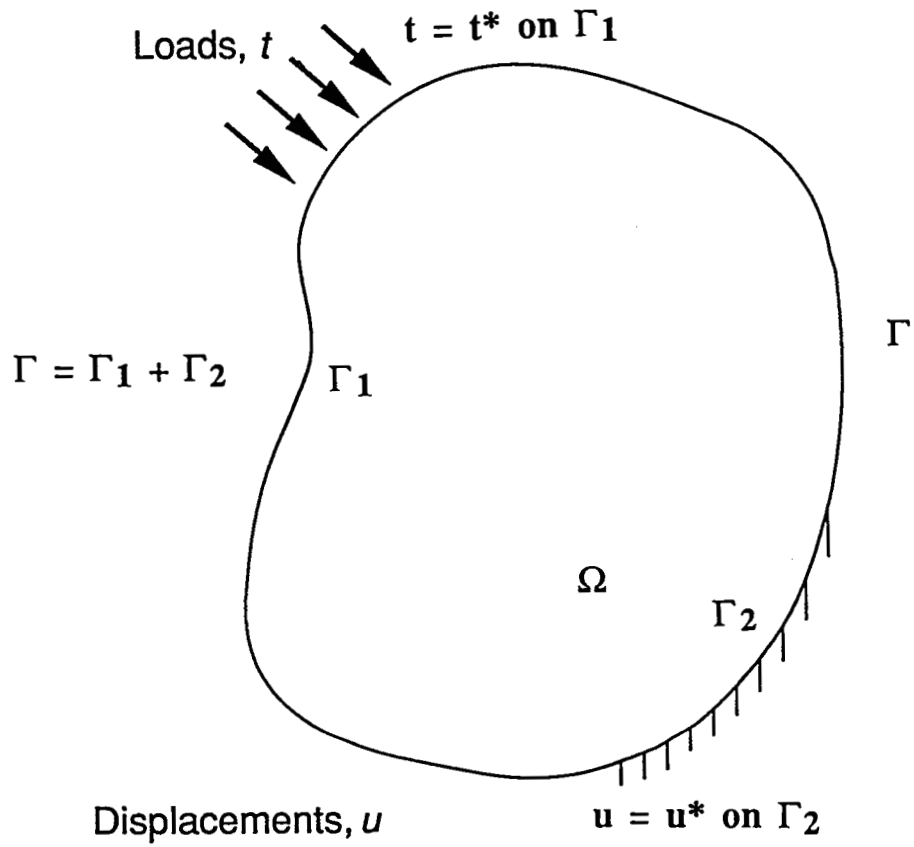


Figure 7. Arbitrary loaded component.

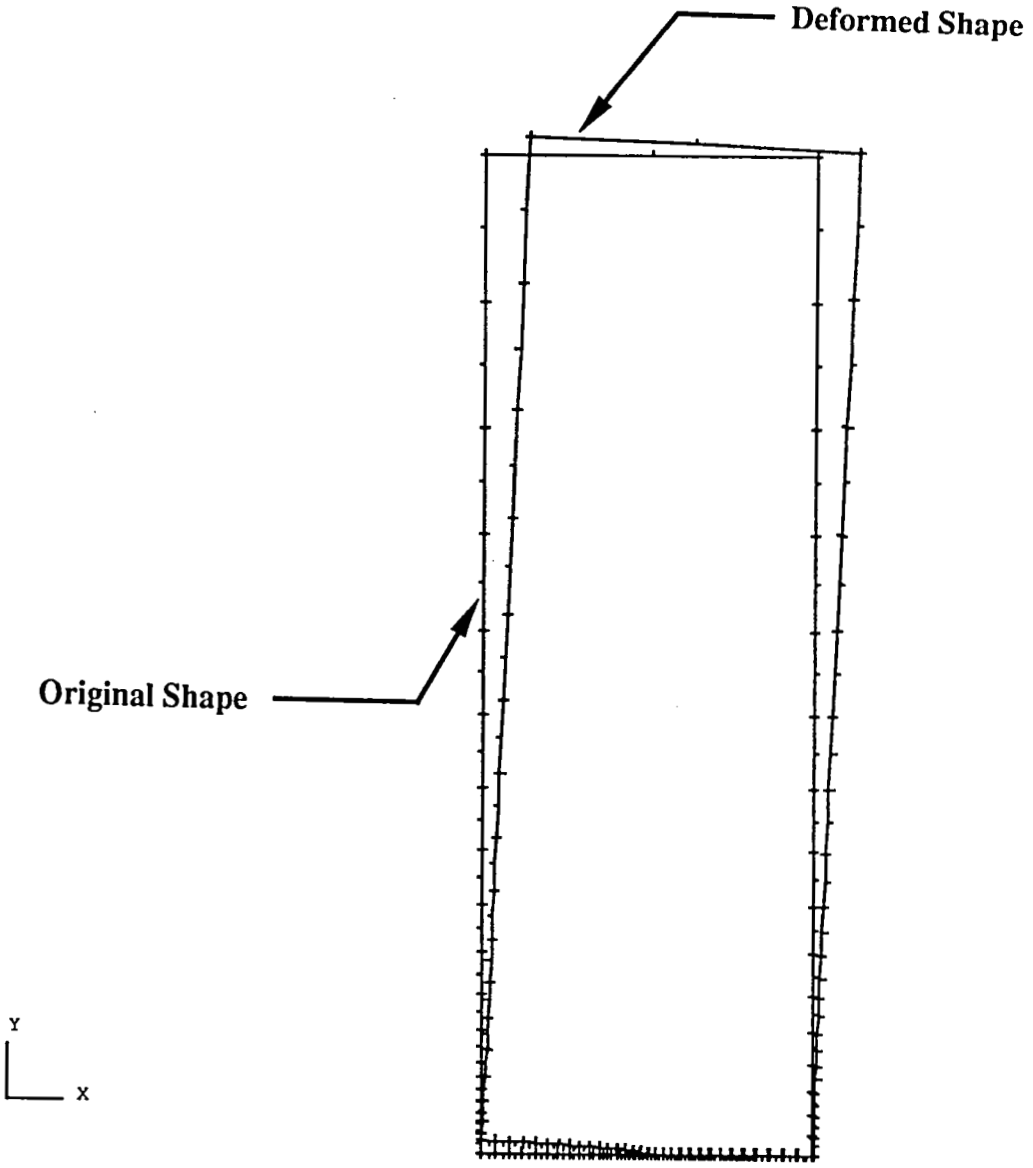


Figure 8. Deformed shape on original shape.

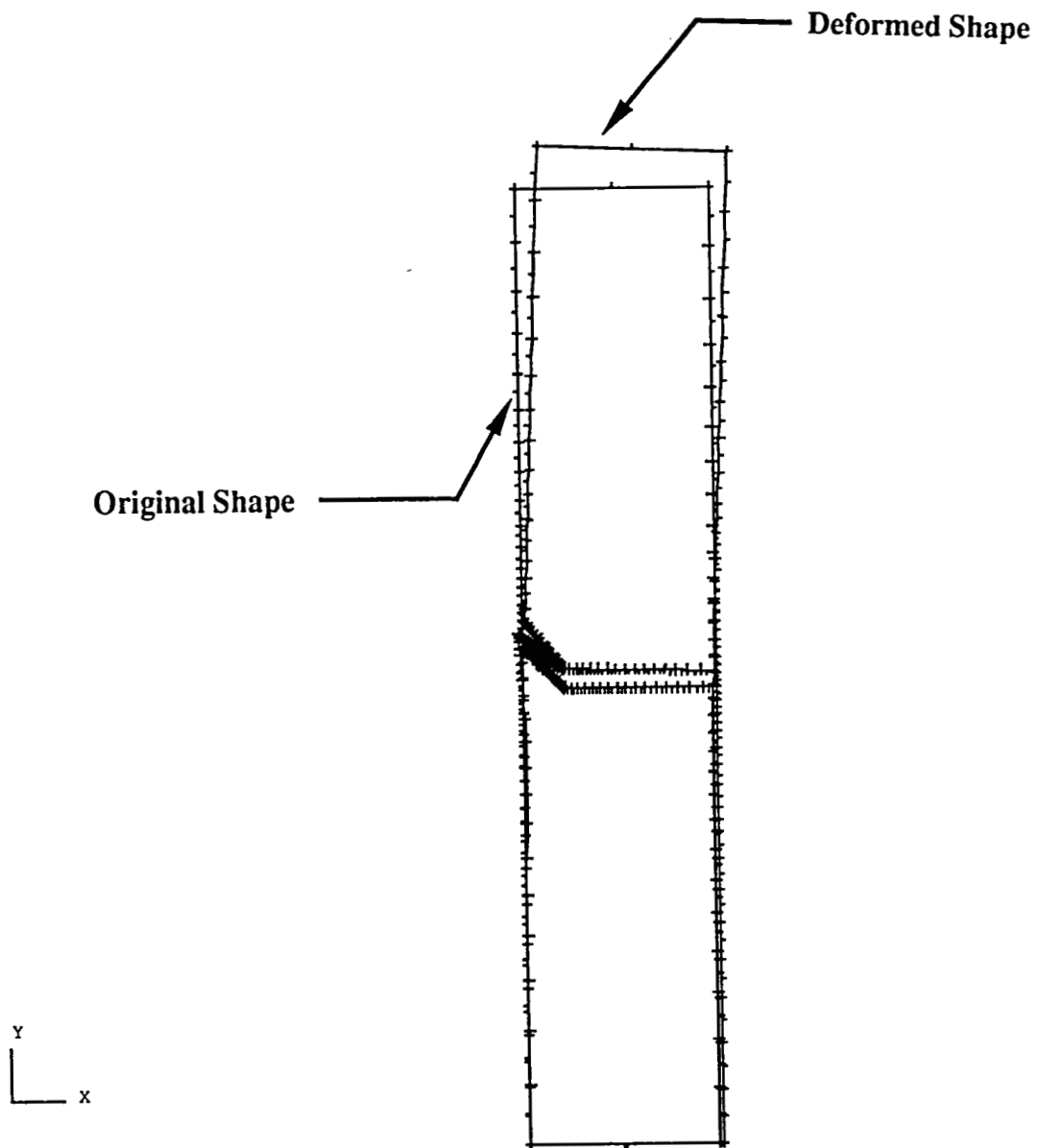


Figure 9. Deformed shape on original shape.

## REFERENCES

1. Barsoum, R.S.: "On the Use of Isoparametric Finite Element in Linear Fracture Mechanics." *Internat. J. Numer. Methods Engrg.*, vol. 10, 1976, pp. 25–37.
2. Benzley, S.E.: "Representation of Singularities With Isoparametric Finite Elements." *Internat. J. Numer. Methods Engrg.*, vol. 8, 1974, pp. 537–545.
3. Cruse, T.A.: "Two-Dimensional B.I.E. Fracture Mechanics Analysis." *Appl. Math. Modeling*, vol. 2, 1978, pp. 287–293.
4. Blandford, G.E., Ingraffea, A.R., and Liggett, J.A.: "Two-Dimensional Stress Intensity Factor Computations Using the Boundary Element Method." *Internat. J. Numer. Methods Engrg.*, vol. 47, 1981, pp. 387–404.
5. Freese, C.F., and Tracey, D.M.: "The Natural Isoparametric Triangle Versus Collapsed Quadrilateral for Elastic Crack Analysis." *Internat. J. Fracture*, vol. 12, 1976, pp. 767–770.
6. Henshell, R.D., and Shaw, K.G.: "Crack Tip Finite Elements Are Unnecessary." *Internat. J. Numer. Methods Engrg.*, vol. 9, 1975, pp. 495–507.
7. Lu, Y.Y., Belytschko, T., and Liu, W.K.: "A Variationally Coupled FE-BE Methods for Elasticity and Fracture Mechanics." *Comput. Methods Appl. Mech. Engrg.*, vol. 85, 1991, pp. 21–37.
8. Atluri, S.N. (ed.): "Computational Methods in the Mechanics of Fracture—Volume 2 in the Computer Methods in Mechanics." Elsevier Science, Amsterdam, The Netherlands, 1986.
9. Knott, J.F.: "Fundamentals of Fracture Mechanics." Butterworth, London, 1973.
10. Paris, P.C., and Sih, G.C.: "Stress Analysis of Cracks." *Fracture Toughness and Testing and Its Applications*, ASTM, Philadelphia, STP 381, 1965, pp. 30–83.
11. Cherpanov, G.P.: "Mechanics of Brittle Fracture." McGraw-Hill, New York, 1979.
12. Sih, G.C., and Liebowitz, H.: "Mathematical Theories of Brittle Fracture." *Fracture: An Advanced Treatise*, vol. 2, H. Liebowitz (ed.), Academic Press, New York, 1968, pp. 68–188.
13. Tong, P., and Pian, T.H.H.: "On the Convergence of the Finite Element Method for Problems With Singularity." *Internat. J. Solids and Structures*, vol. 9, 1973, pp. 313–321.
14. ANSYS 4.4A User's Manuals, vol. I and II, SASI, 1990.
15. Hibbitt, H.D.: "Some Properties of Singular Isoparametric Elements." *Inter. J. for Numer. Methods in Engrg*, vol. 11, 1977, pp. 180–184.
16. Barsoum, R.S.: "Triangular Quarter-Point Elements as Elastic and Perfectly-Plastic Crack Tip Elements." *Inter. J. for Numer. Methods in Engrg.*, vol. 11, 1977, pp. 85–98.

17. Ingraffea, A.R., and Manu, C.: "Stress Intensity Factor Computation in Three Dimensions With Quarter-Point Elements. *Inter. J. for Numer. Methods in Engrg.*, vol. 15, 1980, pp. 1427–1445.
18. Peano, A., and Pasini, A.: "A Warning Against Misuse of Quarter-Point Elements." *Inter. J. for Numer. Methods in Engrg.*, vol. 18, 1982, pp. 314–320.
19. Thompson, G.M., and Whiteman, J.R.: "Analysis of Strain Representation in Linear Elasticity by Both Singular and Nonsingular Finite Elements." *Numer. Methods for Partial Diff. Equations*, vol. 2, 1985, pp. 85–104.
20. Chan, S.K., et al.: "On the Finite Element Method in Linear Fracture Mechanics." *Engineering Fracture Mechanics*, vol. 2, 1970, pp. 1–17.
21. Banks-Sills, L., and Sherman, D.: "Comparison of Methods for Calculating Stress Intensity Factors With Quarter-Point Elements." *Int. J. Fracture*, vol. 32, 1986, pp. 127–140.
22. Wilson, W.K.: "Combined Mode Fracture Mechanics." Ph.D. Dissertation, School of Engineering, University of Pittsburgh, 1969.
23. Owen, D.R.J., and Fawkes, A.J.: "Engineering Fracture Mechanics: Numerical Methods and Applications." Pineridge Press Ltd., Swansea, 1983.
24. BEASY User Guide, Computational Mechanics BEASY Ltd., Version 3.4, 1990.
25. Brebbia, C.A., and Dominguez, J.: "Boundary Elements, An Introductory Course." Computational Mechanics Publications, Southampton, 1989.
26. Irwin, G.R.: "Fracture." *Encyclopaedia of Physics*, S. Flugge (ed.), vol. 6, Springer Verlag, Berlin, 1958.

REPORT DOCUMENTATION PAGE			Form Approved OMB No. 0704-0188	
Public reporting burden for this collection of information is estimated to average 1 hour per response, including the time for reviewing instructions, searching existing data sources, gathering and maintaining the data needed, and completing and reviewing the collection of information. Send comments regarding this burden estimate or any other aspect of this collection of information, including suggestions for reducing this burden, to Washington Headquarters Services, Directorate for Information Operations and Reports, 1215 Jefferson Davis Highway, Suite 1204, Arlington, VA 22202-4302, and to the Office of Management and Budget, Paperwork Reduction Project (0704-0188), Washington, DC 20503.				
1. AGENCY USE ONLY (Leave blank)	2. REPORT DATE August 1992	3. REPORT TYPE AND DATES COVERED Technical Paper		
4. TITLE AND SUBTITLE Applications of FEM and BEM in Two-Dimensional Fracture Mechanics Problems			5. FUNDING NUMBERS	
6. AUTHOR(S) J.B. Min, B.E. Steeve, and G.R. Swanson				
7. PERFORMING ORGANIZATION NAME(S) AND ADDRESS(ES) George C. Marshall Space Flight Center Marshall Space Flight Center, Alabama 35812			8. PERFORMING ORGANIZATION REPORT NUMBER M-695	
9. SPONSORING/MONITORING AGENCY NAME(S) AND ADDRESS(ES) National Aeronautics and Space Administration Washington, DC 20546			10. SPONSORING/MONITORING AGENCY REPORT NUMBER NASA TP-3277	
11. SUPPLEMENTARY NOTES Prepared by the Structures and Dynamics Laboratory, Science and Engineering Directorate.				
12a. DISTRIBUTION / AVAILABILITY STATEMENT Unclassified — Unlimited Subject Category: 39			12b. DISTRIBUTION CODE	
13. ABSTRACT (Maximum 200 words)  A comparison of the finite element method (FEM) and boundary element method (BEM) for the solution of two-dimensional plane strain problems in fracture mechanics is presented in this paper. Stress intensity factors (SIF's) were calculated using both methods for elastic plates with either a single-edge crack or an inclined-edge crack. In particular, two currently available programs, ANSYS for finite element analysis and BEASY for boundary element analysis, were used.				
14. SUBJECT TERMS Linear Elastic Fracture Mechanics (LEFM), Crack-Tip, Singularity, Stress Intensity Factor, Finite Element Method (FEM), Boundary Element Method (BEM)			15. NUMBER OF PAGES 24	16. PRICE CODE A03
17. SECURITY CLASSIFICATION OF REPORT Unclassified	18. SECURITY CLASSIFICATION OF THIS PAGE Unclassified	19. SECURITY CLASSIFICATION OF ABSTRACT Unclassified	20. LIMITATION OF ABSTRACT Unlimited	